Nissen-Meyer, J., Raal, A. J., & Nes, I. F. (1981) *J. Biol. Chem. 256*, 7985-7989.
Panayotatos, N., & Wells, R. D. (1981) *Nature (London) 289*, 466-470.
Rhodes, D., & Klug, A. (1980) *Nature (London) 286*, 573-578.
Riggs, A. D., Bourgeois, S., & Cohn, M. (1970) *J. Mol. Biol. 53*, 401-417.
Schiff, R. D., & Grandgenett, D. P. (1978) *J. Virol. 28*, 279-291.
Schiff, R. D., & Grandgenett, D. P. (1980) *J. Virol. 36*, 889-893.
Schmitz, A., & Galas, D. J. (1980) *Nucleic Acids Res. 8*, 487-506.
Shimotohno, K., Mizutani, S., & Temin, H. M. (1980) *Nature (London) 285*, 550-554.
Shoemaker, C., Goff, S., Gilboa, E., Paskind, M., Mitra, S. W., & Baltimore, D. P. (1980) *Proc. Natl. Acad. Sci. U.S.A. 77*, 3932-3936.
Strauss, H. S., Boston, R. S., Record, M. T., & Burgess, R. R. (1981) *Gene 13*, 75-87.
Sutcliffe, J. G. (1978a) *Cold Spring Harbor Symp. Quant. Biol. 43*, 77-90.
Sutcliffe, J. G. (1978b) *Nucleic Acids Res. 5*, 2721-2728.
Sutcliffe, J. G., Shinnick, T. M., Verma, I. M., & Lerner, R. A. (1980) *Proc. Natl. Acad. Sci. U.S.A. 77*, 3302-3306.
Swanstrom, R., DeLorbe, W. J., Bishop, J. M., & Varmus, H. E. (1981) *Proc. Natl. Acad. Sci. U.S.A. 78*, 124-128.
Tegtmeyer, P., Rundell, K., & Collins, J. (1975) *J. Virol. 16*, 169-178.
Tegtmeyer, P., Lewton, B. A., DeLucia, A. L., Wilson, V. G., & Ryde, K. (1983) *J. Virol. 46*, 151-161.
Van Beveren, C., Goddard, J. G., Berns, A., & Verma, I. M. (1980) *Proc. Natl. Acad. Sci. U.S.A. 77*, 3307-3311.
Winter, R. B., & von Hippel, P. H., (1981) *Biochemistry 20*, 6948-6977.
Yamamoto, T., de Crombrugghe, B., & Pastan, I. (1980) *Cell (Cambridge, Mass.) 22*, 787-797.

Structural Studies of Apolipoprotein A-I/Phosphatidylcholine Recombinants by High-Field Proton NMR, Nondenaturing Gradient Gel Electrophoresis, and Electron Microscopy†

Christie G. Brouillette, James L. Jones, Thien C. Ng, Henri Kercret, B. Hong Chung, and Jere P. Segrest*

ABSTRACT: Complexes formed between apolipoprotein A-I (apo A-I) and dimyristoylphosphatidylcholine (DMPC) or egg phosphatidylcholine have been studied by high-field ^{1}H NMR, nondenaturing gradient gel electrophoresis, electron microscopy, and gel filtration chromatography. Emphasis has been placed on an analysis of the particle size distribution within the micellar complexes produced at lipid/protein molar ratios of 40-700. As determined by electron microscopy and gel filtration of DMPC/apo A-I complexes, the size of the discoidal micelles produced appears to increase uniformly with an increasing lipid/protein ratio. By electron microscopy, the diameters of isolated DMPC/apo A-I discoidal micelles range from approximately 89 Å at a 40 molar ratio to 205 Å at a 700 molar ratio. Analysis of the micellar complexes by ^{1}H NMR shows that concomitant with the increase in size is the progressive downfield shift of the choline *N*-methyl proton resonance of the complex which is observed from 3.245 to 3.267 ppm over the above molar ratio range. The relationship between chemical shift and micelle size is most simply interpreted as arising from a weighted averaging of two lipid environments—lipid–lipid and lipid–protein. In contrast to the above interpretation of the gel filtration experiments on DMPC/apo A-I complexes, nondenaturing gradient gel electrophoresis analysis of particle size distribution leads to an unexpected observation: as the DMPC/apo A-I ratio increases, discrete complexes of increasing size are formed in an apparently quantized manner. A mechanism is proposed for this incremental increase in size that involves a combination of conservative changes in the stoichiometry and conformation of the lipid-associating domains (amphipathic helices) of apo A-I.

The lipid-associating properties of apolipoprotein A-I, the major protein of high-density lipoprotein (HDL),[1] have been widely studied both as a specific model for assessing the structure and function of HDL and as a general model for investigating protein–lipid interactions. A widely studied model system is apolipoprotein A-I/DMPC (Middelhoff et al., 1976; Pownall et al., 1978; Swaney & Chang, 1980; Morrisett et al., 1977; Jonas et al., 1977; Tall et al., 1977). In this system, apo A-I interacts spontaneously with aqueous dispersions of DMPC near the gel to liquid-crystalline phase transition to form small micellar complexes. The ability of apo A-I to spontaneously associate and form stable complexes with phospholipid is a phenomenon observed with exchangeable

† From the Departments of Pathology and Biochemistry, University of Alabama in Birmingham Medical Center, Birmingham, Alabama 35294. *Received June 2, 1983.* This research was supported in part by Grants HL 19551 and HL 28388 from the National Institutes of Health. J.L.J. is a postdoctoral trainee supported by Grant CA 09128 from the National Institutes of Health. NMR facilities were supported by Comprehensive Cancer Center Grant CA 13148 from the National Institutes of Health.

[1] Abbreviations: apo, apolipoprotein; DMPC, dimyristoylphosphatidylcholine; EM, electron microscopy; HDL, high-density lipoprotein; ^{1}H NMR, proton nuclear magnetic resonance; LCAT, lecithincholesterol acyltransferase; MLV, multilamellar vesicle(s); PAGE, polyacrylamide gel electrophoresis; PC, phosphatidylcholine; SUV, small unilamellar vesicle(s); Tris, tris(hydroxymethyl)aminomethane; EDTA, ethylenediaminetetraacetic acid; SDS, sodium dodecyl sulfate.

0006-2960/84/0423-0359$01.50/0

apolipoproteins (apolipoproteins A-I, A-II, C-I, C-II, C-III, and E) and is attributed to their potential to form amphipathic α-helical regions (Segrest et al., 1974; 1976; Segrest & Feldmann, 1977) which insert into a lipid bilayer, sometimes leading to its disruption.

By electron microscopy (Forte et al., 1971) and low-angle X-ray scattering (Atkinson et al., 1976), the small complexes formed between DMPC and apo A-I appear discoidal in shape. Low-angle neutron scattering studies (Wlodawer et al., 1979; Atkinson et al., 1980) support a model (Segrest, 1977) of the complex wherein a disk of lipid bilayer is encircled by the amphipathic helical domains of apo A-I, thereby stabilizing the otherwise exposed fatty acyl chains of the lipids. The study of these discoidal recombinant particles is believed to have physiological relevance since nascent HDL synthesized in the liver (Hamilton et al., 1976) and gut (Green et al., 1978) as well as mature HDL of patients with either heritable or acquired deficiency of LCAT (Norum et al., 1975) also appears to be disks of similar size and shape to the recombinant complexes. Further, it has been demonstrated that discoidal particles prepared from apolipoprotein A-I, cholesterol, and a pure phospholipid, including DMPC, serve as effective substrates for LCAT and can be converted by this enzyme to spheroidal particles not unlike circulating HDL (Matz & Jonas, 1982b; Pownall et al., 1982).

It has been demonstrated that the stoichiometry as well as the size and shape of the resulting complex critically depends on the initial concentrations of protein and lipid as well as the physical state of the lipid (Swaney, 1980; Jonas et al., 1980, 1981). Swaney (1980) has shown, using chemical cross-linking reagents, that over the range of DMPC/apo A-I molar ratios of 20–600 two kinds of micellar complexes are produced that have either two or three apo A-I molecules per particle. The dimer complexes are produced at every ratio, but the trimer predominates at the higher DMPC/apo A-I ratios. Jonas et al. (1980) have reported that at high DMPC/apo A-I molar ratios (>500), stable, apparently vesicular complexes are formed in addition to micellar complexes. In the above studies, the products obtained appeared to be relatively homogeneous by gel filtration chromatography. We report here, through the use of gradient gel electrophoresis and negative stain electron microscopy, that each class of micellar complex produced from the interaction of apo A-I with DMPC is actually composed of discrete and well-defined species which we have characterized by particle size. In contrast to what may be deduced by gel filtration chromatography, as the DMPC/apo A-I ratio in the product mixture is increased, the appearance of species of increasing particle size occurs in a discontinuous fashion which we believe is a result of a combination of changes in the apo A-I stoichiometry and conformation in the particle.

In the present study, we have also employed high-field ^{1}H NMR to explore the phospholipid head group structure in discrete DMPC/apo A-I complexes. We have previously reported (Brouillette et al., 1982) that the chemical shift of the phospholipid *N*-methyl resonance is a very sensitive indicator of the head group surface area, which, in turn, is related to a combination of the head group conformation and/or hydration. In this study, we conclude that the phospholipids around the perimeter of a discoidal micelle are in a different chemical environment that the core phospholipid due to the presence of protein and/or the absence of lipid.

Experimental Procedures

Preparation of Apolipoprotein A-I. Plasma HDL (d = 1.063–1.210 g/mL) was isolated from fresh normolipidemic plasma by the sequential flotation method using KBr for density adjustment (Havel et al., 1955). The isolated HDL was washed once by reisolation in KBr solution of the same density and then dialyzed exhaustively against 0.15 M NaCl/0.01% EDTA, pH 7.4. Apo HDL was prepared by delipidating the lyophilized HDL with ether/ethanol (3:1 v/v), and apo A-I was then separated from the apo HDL by a combination of gel filtration and ion-exchange chromatography (Edelstein et al., 1973). The purity of isolated apo A-I was determined by urea (Kane, 1973) and SDS (King & Laemmli, 1971) gel electrophoresis.

Preparation of Small Unilamellar Vesicles. Dimyristoylphosphatidylcholine in ethanol was obtained from Avanti Polar Lipids, Inc. (Birmingham, AL). After the removal of solvent by evaporation under reduced pressure, followed by a 50 μmHg vacuum treatment for 8 h, the dried lipid was suspended in either a D_2O or a H_2O buffer (0.1 M Tris, 0.15 M NaCl, and 0.02% NaN_3, pH 8.0), depending on the ultimate chromatographic procedure, at a concentration between 15 and 20 mg/mL and sonicated at 28 °C under N_2. Low-speed centrifugation was used to remove sonicator probe tip particles that might be present. The mean Stokes radius, determined by gel filtration chromatography on Sephacryl 400 (Brouillette et al., 1982) of the DMPC SUV, was approximately 120 Å.

Formation and Isolation of Protein/Lipid Complexes. A solution of apo A-I in 0.01 M Tris, 0.15 M NaCl, and 0.02% NaN_3, pH 8.0, was added to DMPC SUV (~15 mg/mL) at the appropriate initial molar ratio desired and incubated at 24 °C for 24 h. Following incubation, a 1-mL aliquot of the mixture, containing no less than 10 mg of DMPC, was applied to a 1.2 × 95 cm Sephacryl 400 (or Sepharose 4B) column and eluted at room temperature with a H_2O or D_2O buffer (0.01 M Tris, 0.15 M NaCl, and 0.02% NaN_3, pH 8.0). Fractions of 1 mL were collected at a flow rate of 4 mL/h and utilized in subsequent experiments within 24 h. Samples eluted with the H_2O buffer were dialyzed against the D_2O buffer prior to NMR measurements. Phospholipid concentration was determined by the method of Stewart (1980) or by the incorporation of [^{14}C]DMPC. Protein concentration was determined by the method of Lowry et al. (1951).

To prepare egg PC/apo A-I complexes at a 40 molar ratio, 0.5 mL of 0.54 M sodium deoxycholate in 0.01 M Tris, 0.15 M NaCl, and 0.02% NaN_3, pH 8.0, was added to a dry film of 25 μmol of egg phosphatidylcholine (Avanti Polar Lipids, Inc.). After being thoroughly mixed, a 6 μM solution of apo A-I in the above buffer was added. This mixture was dialyzed exhaustively prior to gel filtration or gradient gel electrophoresis. ^{1}H NMR samples were prepared as described above.

^{1}H NMR Spectroscopy. All proton NMR spectra were measured with a Bruker WH400 spectrometer. A 5-mm probe incorporated with a BVT-1000 air flow temperature-controlled unit was used throughout the experiment and thermostated at 25 ± 0.5 °C. A 45° pulse of 8 μs and a repetition rate of 2 s were used to sample the signal. Under these conditions, no saturation of the resonances was observed. The number of scans was varied from 16 to 128, depending on the signal to noise ratio. For aqueous or high water containing solutions, the selective, gated saturation technique was employed to suppress the water resonance. Under the conditions used, no saturation transfer to the choline *N*-methyl resonances was observed. A 0.4-Hz line broadening was applied to each FID prior to the Fourier transform. Convolution difference spectra were obtained by applying 0.2- and 5-Hz line broadening (Campbell et al., 1973). Sodium 3-(trimethylsilyl)-propionate-*2,2,3,3-d*$_4$ was used as an internal standard.

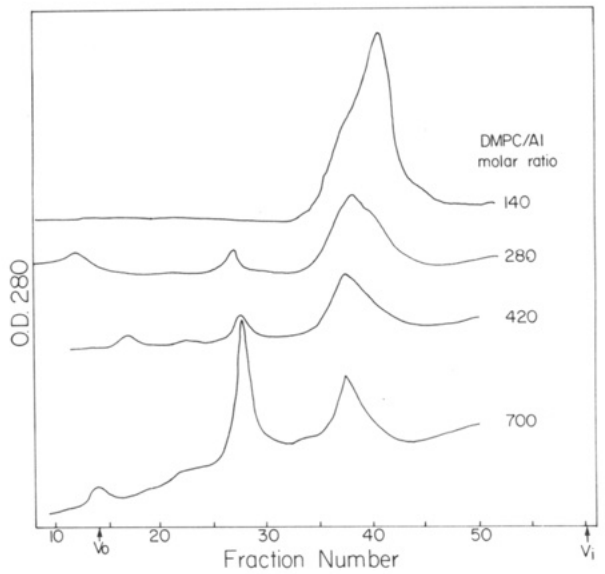

FIGURE 1: Elution profiles from Sepharose 4B chromatography of DMPC/apo A-I product mixtures at the indicated molar ratios. Preparations were incubated at 25 °C for 24 h, followed by gel filtration.

Gradient Gel Electrophoresis. A 12 × 14 cm gradient slab gel was formed from a 4–25% linear gradient of acrylamide, pH 8.3. A 3% stacking gel, pH 8.3, was poured after the resolving gel had polymerized. Electrophoresis was performed at 15 °C in 0.05 M Tris–0.38 M glycine, pH 8.3, at 150 V constant voltage for 36 h. It was determined that the pore-limiting migration position of DMPC/apo A-I complexes was established by 24 h. The gel was fixed and stained with 0.2% Coomassie Brilliant blue, 5% methanol, and 7.5% acetic acid. The protein standards thyroglobulin, ferritin, catalase, lactate dehydrogenase, and bovine serum albumin were used to generate a calibration curve relating Stokes diameter to the electrophoretic R_f, the latter defined as the equilibrium migration distance relative to bovine serum albumin.

Electron Microscopy. The PC/apo A-I complexes, as prepared, were stained with 2% (w/v) potassium phosphotungstate, pH 5.9, and examined with a Philips EM400 microscope on carbon-coated, Formvar grids.

Results

Gel Filtration of DMPC/Apo A-I Complexes. The size and type of complex produced from the interaction of DMPC with apo A-I, as deduced by gel filtration (Swaney, 1980; Jonas et al., 1980), depend on the starting ratio of lipid to protein (Figure 1). At low DMPC to protein ratios (<100 M/M),[2] a single complex is observed by gel filtration. At intermediate DMPC to protein ratios (between 100 and 300 M/M), the elution profile of the complex begins to appear bimodal due to the presence of a second, larger complex in addition to the first one observed. By chemical cross-linking between dimethyl suberimidate and each isolated complex, Swaney (1980) has determined that these complexes contain two and three apo A-I molecules per particle, respectively. Using the same technique, we have also observed that, starting at a molar ratio of approximately 200 DMPC/apo A-I, particles containing both two and three apo A-I molecules are produced (data not shown). At high DMPC to protein ratios (>300 M/M), the chromatogram shows a peak with a retention volume very similar to that for DMPC vesicles alone (fraction 28, Figure 1). However, tryptophan fluorescence measurements, as well as chemical analysis for protein, reveal the presence of protein in this peak. This new complex, in contrast to the two complexes eluting in fractions 37–41, appears vesicular on the basis of ^{1}H NMR data, a possibility confirmed by more detailed ^{1}H NMR analyses of fractionated species (see below).

[2] When given, the molar ratio will refer to the initial molar ratio in the product mixture.

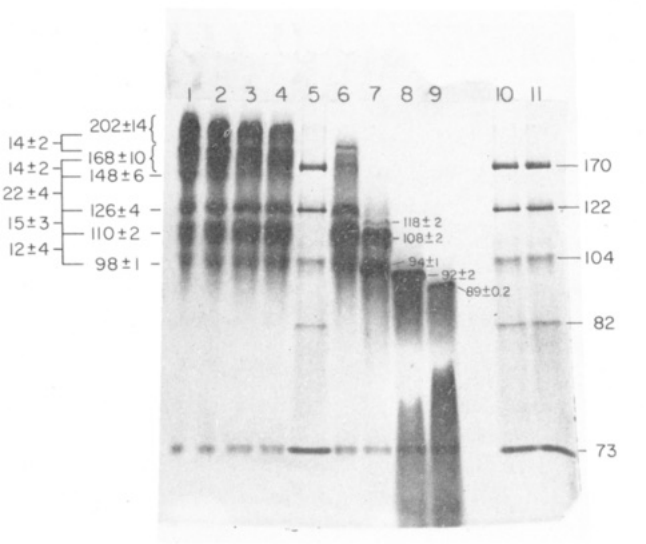

FIGURE 2: Gradient gel electrophoresis of DMPC/apo A-I complexes formed at the following molar ratios: 700 (lane 1), 600 (lane 2), 500 (lane 3), 400 (lane 4), 300 (lane 6), 200 (lane 7), 100 (lane 8), and 40 (lane 9). Standard protein mixtures were electrophoresed in lanes 5, 10, and 11, and their respective Stokes diameters are indicated in lane 11. The calculated Stokes diameter of the major species observed and the difference in diameter between adjacent species are given as the mean (see text for details). The gel was stained with Coomassie brilliant blue. Free apo A-I is apparent in lanes 8 and 9.

Gradient Gel Electrophoresis and Electron Microscopy. Gradient gel electrophoresis creates a continuous gradation in pore size using a linear polyacrylamide gradient which enables uniform resolution over a large range of particle sizes. With five reference proteins of known Stokes radii, a calibration curve is generated relating a protein's R_f (the equilibrium migration distance relative to bovine serum albumin) to its Stokes radius. Using a 4–25% gradient gel, products formed at DMPC/apo A-I molar ratios of 40–700 were electrophoresed under nondenaturing conditions, which ensure migration of the intact protein/lipid complex (Blanche et al., 1981; Nichols et al., 1983). A typical gel is shown in Figure 2. Clearly shown is a quantized heterogeneity of species within each product mixture that is neither observed nor predicted by gel filtration chromatography of the same sample. The observed electrophoretic pattern is reproducible and not a result of decomposition during electrophoresis, a possibility that has been ruled out by reelectrophoresis on a gradient gel in the second dimension. Indicated on the gel pattern shown in Figure 2 is the mean Stokes diameter for each major species observed, obtained from gradient gels run on four different "titration" experiments. The limiting pore size in our gels is estimated to be a Stokes diameter of approximately 250 Å, which prevents anything larger from entering the gel. For example, at a 700 DMPC/apo A-I ratio (M/M), products elute in two different peaks by gel filtration, as shown in Figure 1, centered at fractions 28 and 38. However, the gradient gel electrophoretic profile of the entire product mixture is essentially identical with the profile of the pooled fractions centered at fraction 38, indicating that the larger complexes do not enter the gel. Additionally, we have found the electrophoretic pattern to be the same for product mixtures prepared from

apo A-I and either DMPC SUV or MLV. The observed gradient gel species have been grouped into two major classes (designated R-2 and R-3) for the following reasons: (1) As depicted on the far left side of Figure 2, there is a fairly constant quantized increase in diameter of 12–15 Å between adjacent species on the gel. There is only one exception, and this can be seen as a clear break in the gel pattern which measures 22 ± 4 Å. (2) As discussed above, the gradient gels depict particle size heterogeneity within the micellar complexes formed in the various product mixtures. With this in mind, the initial appearance of the larger micellar complex observed by gel filtration corresponds with the initial appearance of the R-3 class of particles observed by gradient gel electrophoresis. The initial appearance of R-3 species detected by gradient gel electrophoresis varies between 200 and 300 DMPC/apo A-I (M/M). This is consistent with our observation and Swaney's (1980) observation that both two and three apo A-I complexes are produced in this concentration range. The class designations of R-2 and R-3 refer, therefore, to the presumptive apo A-I stoichiometry within each class of micellar complexes.

Negative stain electron microscopy was used as an alternate method of analyzing the particle size heterogeneity of the product mixtures. It was also important to confirm that the particle size distribution observed by gradient gel electrophoresis was present in the starting product mixture and not, therefore, produced by electrophoresis. Additionally, since the entire sample can be visualized, information on the species larger than the micellar complexes is available from studying electron micrographs of the appropriate product mixtures. The data from several DMPC/apo A-I product mixtures with molar ratios of 40–700 are presented in the form of histograms in Figure 3A–E, along with representative electron micrographs. To illustrate reproducibility between preparations run at the same molar ratio, histograms of particle size distribution from two different product mixtures are superimposed for the molar ratios 100 and 700. Also included (Figure 3E) are data obtained from a single gel filtration column fraction of the predominant micellar complex formed at a DMPC/apo A-I molar ratio of 700. In Figure 3F, a plot of mean particle size as a function of DMPC/apo A-I molar ratio is derived from the data in panels A–D along with data from additional molar ratios. A good correlation between particle sizes measured by gradient gel electrophoresis and electron microscopy is seen, even though the necessary assumption that the complexes are spherical during electrophoresis may cause a slight underestimate of their Stokes diameter. For example, (1) by gradient gel electrophoresis, product mixtures of DMPC/apo A-I at molar ratios of 40 and 100 are very homogeneous with particle mean Stokes diameters of 89 ± 0.2 and 92 ± 2 Å, respectively. The electron micrographs of these mixtures are also quite homogeneous with average particle diameters of 85 ± 9 and 100 ± 10 Å, respectively. (2) At a molar ratio of 300, where a significant number of R-3 as well as R-2 complexes are produced, diameters determined by gradient gel electrophoresis range from 97 ± 1 to 202 ± 4 Å. By electron microscopy, the particles appear polydisperse; 95% of the particles range in size between 90 and 215 Å in diameter. (3) At molar ratios of 400 and greater, a notable fraction of the products elutes earlier than the micellar complexes by gel filtration but is too large to enter the gradient gel. These larger complexes do appear in the electron micrographs, however. (4) Gel filtration of the 700 molar ratio product mixture shows that the predominant micellar class is the larger of the two produced. By gradient gel electrophoresis, the majority of the species are found in the R-3 class and range in size from 148 ± 6 to 202 ± 14 Å in diameter. The electron micrograph of the predominant micellar complex isolated by gel filtration shows a mean diameter of 205 ± 24 Å (Figure 3E).

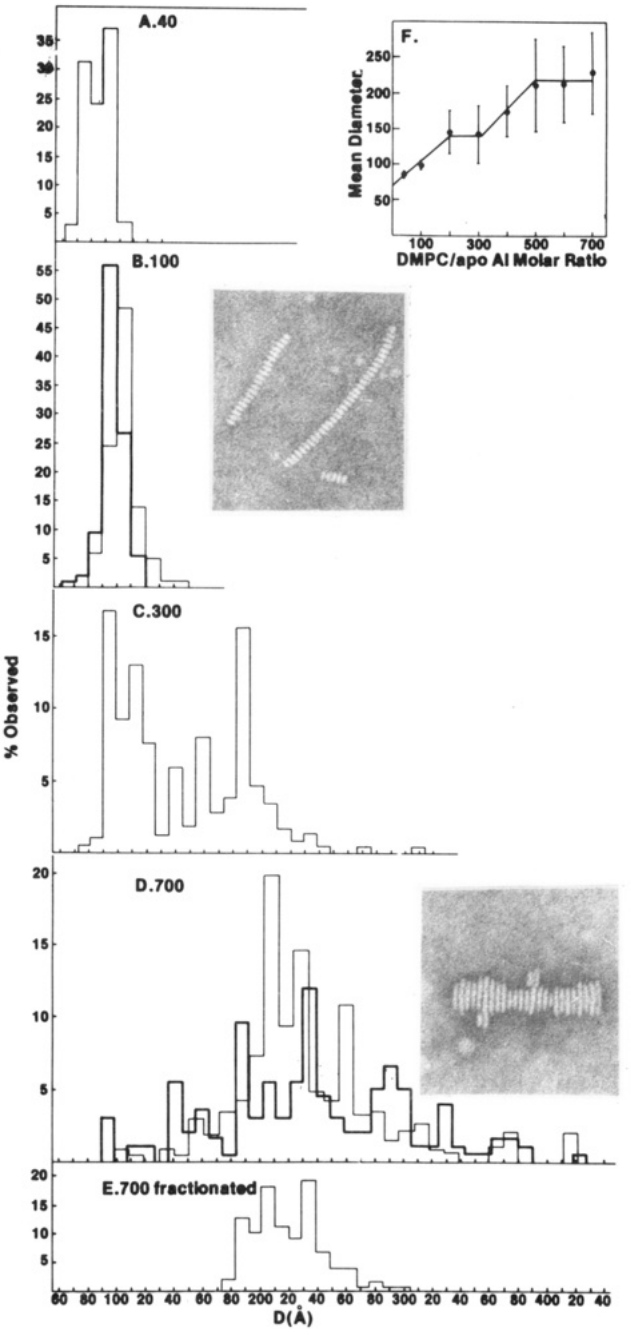

FIGURE 3: Particle size distribution obtained from electron micrographs of negatively stained DMPC/apo A-I product mixtures at the following molar ratios: (A) 40, number of particles measured (n) = 54; (B) 100, n = 108 for dark-line histogram, n = 104 for light-line histogram; (C) 300, n = 283; (D) 700, n = 383 for dark-line histogram, n = 198 for light-line histogram; (E) a single column fraction of the predominant micellar complex produced at a 700 molar ratio, n = 182. (F) Overall mean particle size as a function of DMPC/apo A-I molar ratio: 200, n = 248; 400, n = 187; 500, n = 191; 600, n = 184. Bars indicate the standard deviation. Measurements were made on particles oriented in rouleaux; electron microscopic magnification is 147680×.

^{1}H NMR of DMPC/Apo A-I Complexes. (A) Formation of DMPC/Apo A-I Complexes. In DMPC SUV, two choline *N*-methyl proton resonances are observed at 3.285 and 3.248 ppm, corresponding to lipids residing in the outer (downfield) and inner monolayer, respectively (Figure 4A). When apo A-I is incubated with DMPC SUV, the complex formed displays a ^{1}H NMR spectrum qualitatively very similar to that

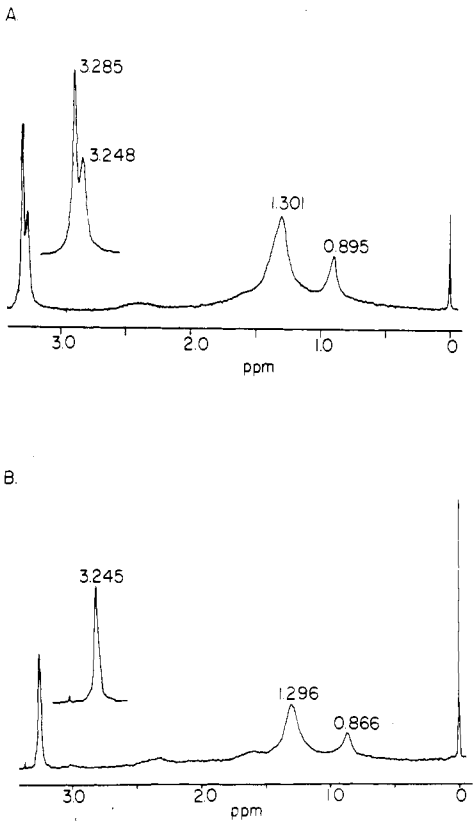

FIGURE 4: ^{1}H NMR spectra of (A) DMPC small unilamellar vesicles and (B) the DMPC/apo A-I complex formed at a molar ratio of 40. To a suspension of DMPC vesicles was added an aliquot of apo A-I in solution; the preparation was incubated at 25 °C for 1 h before the ^{1}H NMR spectrum was recorded.

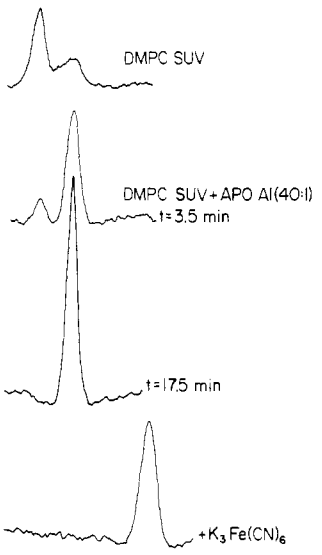

FIGURE 5: Kinetics of the interaction of apo A-I with DMPC small unilamellar vesicles at a molar ratio of 40. The chemical shift of the deconvoluted choline *N*-methyl region was used to monitor the progress.

of DMPC SUV alone, with the notable exception of the phosphatidylcholine *N*-methyl resonance, which is now a single peak (Figure 4B), the exact chemical shift of which depends on the DMPC/apo A-I molar ratio. For a DMPC/apo A-I molar ratio of 40, this transformation is complete in less than 20 min at 25 °C (Figure 5). Addition of the shift reagent $K_3Fe(CN)_6$ results in a complete shift of the new *N*-methyl resonance, suggesting that all the DMPC head groups are now exposed to the bulk solvent (Figure 5). The extent of the

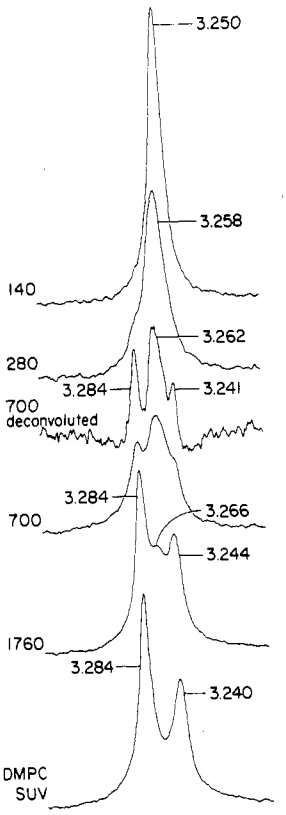

FIGURE 6: ^{1}H NMR spectra of the choline *N*-methyl region of product mixtures obtained from interacting DMPC small unilamellar vesicles with apo A-I, in solution, at the indicated molar ratios. The progress of product formation was monitored by ^{1}H NMR, and the spectrum was recorded after the reaction appeared complete.

conversion can be deduced from the presence of residual SUV resonances (i.e., the characteristic double *N*-methyl proton resonance) in the product mixture spectrum (Figure 6). As the DMPC/apo A-I molar ratios increase between 280 and 420, the spectrum of the product mixture displays resonances indicative of both SUV and complexes, suggesting the incomplete breakdown of the vesicles by apo A-I. These spectra are compatible with and confirm the interpretation of the gel filtration experiments on the product mixtures from which these spectra were recorded (Figure 1). As mentioned above, a distinctive feature in these spectra is a progressive downfield shift of the micelle *N*-methyl resonance with increasing DMPC/apo A-I ratios. The significance of this will be discussed later.

(*B*) *Fractionated DMPC/Apo A-I Complexes.* ^{1}H NMR spectra were obtained on column-fractionated products formed at DMPC/apo A-I molar ratios of 100 and 700 to determine (a) whether the difference in A-I stoichiometry between the predominant micellar complex formed at DMPC/apo A-I molar ratios of 100 vs. 700 (R-2 vs. R-3, respectively) could be detected by a difference in chemical shift of the *N*-methyl resonances of these species, in addition to their demonstrated size difference, and (b) whether the large complexes formed at high DMPC/apo A-I ratios, which are thought to be vesicular, do, in fact, show vesicle-like *N*-methyl resonances similar to those observed in the product mixtures (Figure 6). The *N*-methyl resonance of the micellar complex produced at a 100 molar ratio is observed upfield (3.248 ppm, Figure 7B) from that of the 700 molar ratio (3.267 ppm, Figure 8B). These shift values are close to those observed in the respective product mixtures (Figure 6). As anticipated, the ^{1}H NMR spectrum of fraction 40 obtained from the 700 molar ratio displays SUV-like *N*-methyl resonances at 3.287 and 3.254

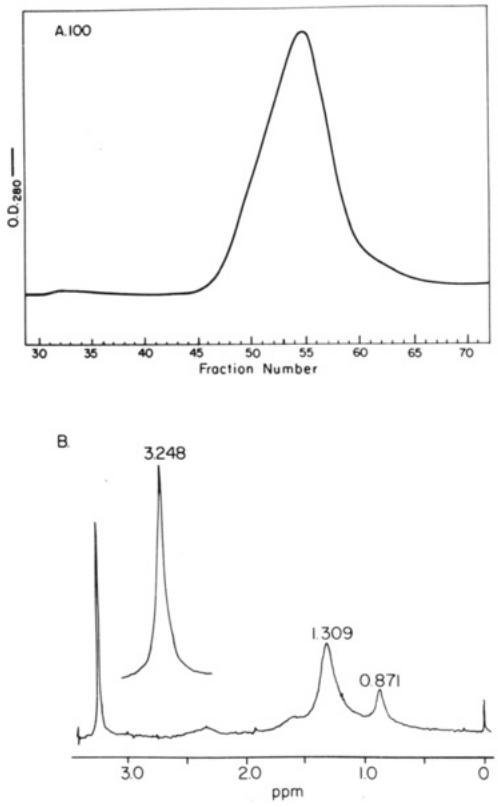

FIGURE 7: Gel filtration on Sephacryl 400 of a 100 M/M DMPC/apo A-I product mixture (V_0 = fraction 31 and V_i = fraction 86) (A) and the ^{1}H NMR spectrum of fraction 55 (B).

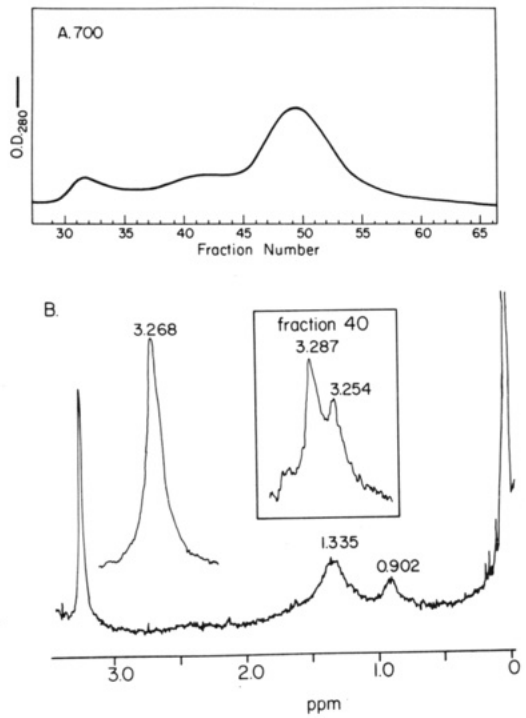

FIGURE 8: Gel filtration on Sephacryl 400 of a 700 M/M DMPC/apo A-I product mixture (V_0 = fraction 31 and V_i = fraction 86) (A) and the entire ^{1}H NMR spectrum of fraction 50 and the choline *N*-methyl region of fraction 40 (B).

ppm (Figure 8B). The chemical shifts of the *N*-methyl proton resonances are quite reproducible both within a given NMR experiment and between experiments. The ^{1}H NMR spectra of the *N*-methyl region obtained from several collected fractions across a micellar complex peak appeared as predominantly a single resonance and were within ±0.001 ppm.

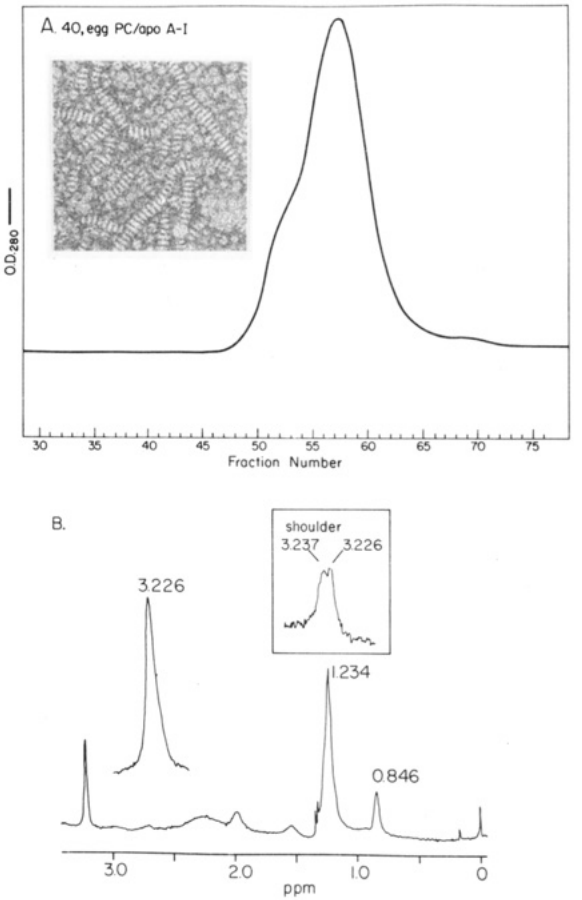

FIGURE 9: Gel filtration on Sephacryl 400 of a 40 M/M egg PC/apo A-I product mixture produced by deoxycholate dialysis (V_0 = fraction 31 and V_i = fraction 86) (A) and the ^{1}H NMR spectrum of the corresponding major and minor (choline *N*-methyl region only) complexes isolated by gel filtration (B). The negative stain electron micrograph is from an unfractionated sample; electron microscopic magnification is 147680×.

Chemical shifts between identical experiments were within ±0.002 ppm. The latter value is obtained from a series of four experiments which were performed over a 2-year period.

Egg PC/Apo A-I Complexes. Micellar complexes that appear morphologically identical by electron microscopy with DMPC/apo A-I discoidal complexes can be produced with egg PC and apo A-I if reconstituted in the presence of a detergent, such as sodium deoxycholate, that is subsequently removed by dialysis or gel filtration (Nichols et al., 1983; Matz & Jonas, 1982a; Pownall et al., 1982). Because of their morphological similarity to nascent HDL and the presence of a more physiologically relevant lipid, egg PC/apo A-I complexes may be a more suitable model for HDL. For these reasons, as well as their similarity to DMPC/apo A-I micellar complexes, we were interested in the ^{1}H NMR spectra and gradient gel electrophoretic pattern of the egg PC/apo A-I complexes. Illustrated in Figure 9A is a gel filtration profile of a 40 molar ratio (egg PC/apo A-I) product mixture prepared by sodium deoxycholate dialysis. An electron micrograph of an unfractionated sample is also shown. The mean diameter measured by electron microscopy is 74 ± 10 Å, a value significantly smaller than the smallest DMPC/apo A-I micellar complex observed. However, the size distribution in this sample is skewed, with the mode centered at 70 Å and approximately 10–20% of the particles measuring 85–100 Å in diameter. Illustrated in Figure 9B is the ^{1}H NMR spectrum of the predominant species isolated by gel filtration. The chemical shift of the choline *N*-methyl resonance is 3.226 ppm.

This chemical shift is upfield of the most upfield shift (3.245 ppm) observed for a DMPC/apo A-I complex. A minor component is detected by gel filtration as a shoulder on the major peak. This component could not be isolated as a pure species, and the ^{1}H NMR of the choline *N*-methyl region of this fraction displayed two resonances at 3.237 and 3.226 ppm (Figure 9B, insert), the latter shift due to contamination by the major species produced. By gradient gel electrophoresis, one major (>90%) and two minor species were seen with Stokes diameters of 73, 79, and 86 Å, respectively.

Discussion

Apolipoprotein A-I interacts with DMPC SUV or MLV near the phase transition of the lipid to produce two structurally distinct complexes: vesicles and discoidal micelles. Micellar complexes are produced at all DMPC/apo A-I ratios, with larger complexes appearing at higher ratios. Vesicular complexes appear at a DMPC/apo A-I molar ratio of approximately 300, and their relative contribution to the product mixture increases with increasing DMPC/apo A-I ratios. The micellar complexes have been shown to be composed of two classes which we have designated R-2 and R-3 on the basis of the apo A-I stoichiometry of 2 or 3 in the individual particles produced (Swaney, 1980). A good deal of information about these complexes has been obtained from gel filtration experiments. We have observed, as others have (Swaney, 1980), that the average size of the R-2 class increases with increasing DMPC/apo A-I ratios. Furthermore, the average size of the R-2 class appears to reach a limit at about a molar ratio of 200 (see Figures 2 and 3F) where the R-3 complex first appears. The R-3 class also varies directly in size with the DMPC/apo A-I ratio (Figures 2 and 3F).

What has not been detected by gel filtration is the dramatic heterogeneity, in the form of discretely quantized sizes, within each given class. This is clearly observed by gradient gel electrophoresis of the DMPC/apo A-I product mixtures. Any method of separation, including gel filtration, used to analyze these products could potentially alter the composition of the preparation in some undetectable manner. However, the excellent qualitative agreement between the gradient gel and electron microscopic analysis of the product size distribution argues against this possibility, as does the stability of the observed gradient gel profile to two-dimensional electrophoresis and the reproducibility of the technique. This technique recently has been utilized to analyze the size distribution of HDL subpopulations (Blanche et al., 1981). Subpopulations identified by gradient gel electrophoresis under nondenaturing conditions correlated well with those obtained from analytical ultracentrifugation. During the course of this work, Nichols et al. (1983) reported a gradient gel electrophoresis study of egg PC/apo A-I complexes prepared by detergent dialysis. The gradient gel electrophoretic pattern they obtained for an egg PC/apo A-I molar ratio of 25 compares well with ours. Their reported R_f values for the three observed species were 0.80, 0.70, and 0.63, while ours are 0.80, 0.68, and 0.61.

As shown by gradient gel electrophoresis (Figure 5), the Stokes diameter of each species produced is highly reproducible, and the distance between species is a constant value of 13 ± 3 Å. This value is the overall mean distance between adjacent species in every lane from four different gradient gels. There is an obvious exception to this mean value which occurs with the appearance of a species separated by a distance of 22 ± 4 Å from the smaller, adjacent species. The appearance of this species coincides with the appearance of the R-3 complex detected by gel filtration chromatography. The results obtained by electron microscopy, illustrated in Figure 3F, are also compatible with the formation of two micelle classes. Although the data in the plot of mean particle diameter vs. DMPC/apo A-I molar ratio (Figure 3F) can be fit to a straight line, a step function would also fit, which levels off at diameters of 140 and 220 Å. These values are close to the limiting diameters of the R-2 and R-3 classes observed by gradient gel electrophoresis (126 and 202 Å, respectively). Furthermore, we believe the electron micrographs display a hint of the quantization within classes observed by gradient gel electrophoresis. Figure 10 is a cumulative plot from electron micrographs of the particle size distribution of DMPC/apo A-I particles for molar ratios of 200–700 in increments of 100. The results represent the combined measurements of two observers (n = 500 + 500). Even though it is not possible to assign a one to one correspondence between particle size measured by gradient gel electrophoresis and particle size measured by electron microscopy, the spikes in the electron microscopic size distribution seem to correspond to the Stokes diameter of most of the gradient gel electrophoretic bands. However, this interpretation is made with caution, since the technical limitations of negative stain electron microscopy enable a measurement of particle diameter to only the nearest 8–9 Å.

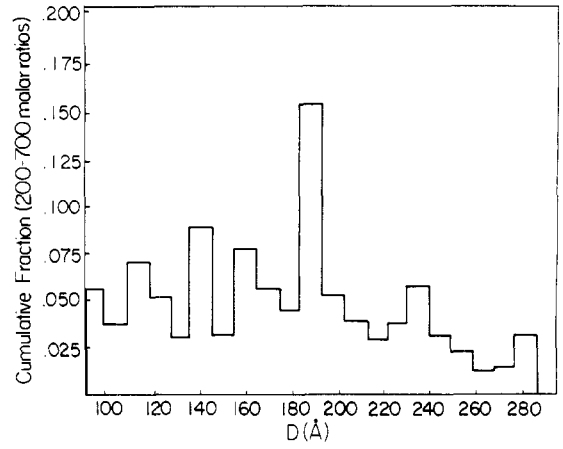

FIGURE 10: Cumulative plot of particle size distribution of DMPC/apo A-I particles for molar ratios 200–700 obtained from electron micrographs. Measurements were made on particles oriented in rouleaux; n = 1000 (see text for details).

As noted by others (Swaney, 1980; Wetterau et al., 1983), the product of association between phospholipid and apo A-I has considerable size flexibility. On the basis of the studies reported here, we propose that the mechanisms for size flexibility are of three kinds: (1) Flexibility of the first kind involves a discontinuous change in the discoidal diameter due to a change in the number of apolipoprotein A-I molecules associated per discoidal complex, i.e., R-2 vs. R-3. (2) Flexibility of the second kind involves discontinuous changes in the diameter of species within a given class (e.g., within R-2). These incremental changes are quantized between adjacent species within each class and are equal to a diameter change of approximately 13 Å (or equivalent to a discoidal circumference change of 40 Å). We believe that each quantized circumference change reflects incremental changes in the number of amphipathic helices per disk edge and is associated with concomitant changes in the number of phospholipid molecules per disk. A 40-Å change in disk circumference is approximately equivalent to either the thickness of two to three antiparallel amphipathic helices (Tall et al., 1977) (right-hand side of Figure 11) or the length of a single, or a parallel pair of, 22-residue amphipathic helices (Segrest, 1977) (left-hand side of Figure 11). (3) Flexibility of the third kind is suggested

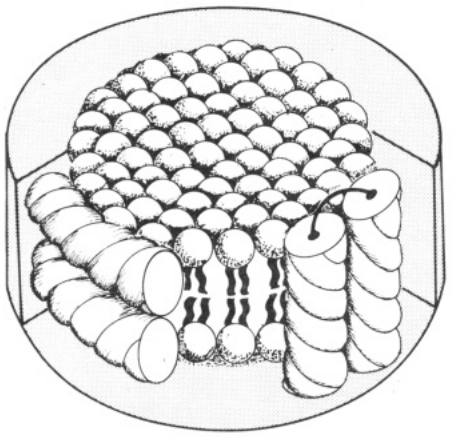

FIGURE 11: Discoidal micelle model for DMPC/apo A-I, illustrating two possible orientations of the amphipathic helices.

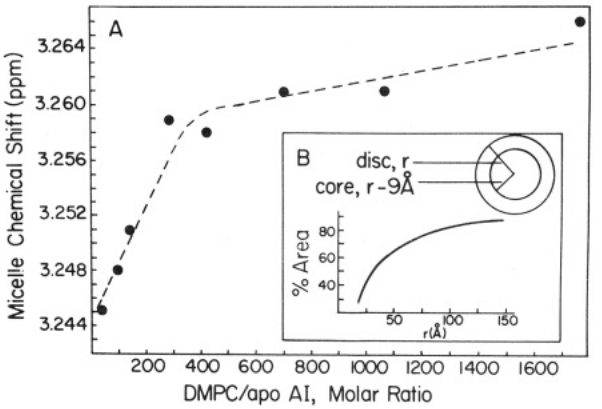

FIGURE 12: Dependence of the micelle choline *N*-methyl proton chemical shift (some of these were taken from spectra of product mixtures as illustrated in Figure 6) on the DMPC/apo A-I molar ratio (A) and the relationship between the percent surface area in the core of a lipid disk and the total surface area of a discoidal particle of varying radius (B). The value indicated on the *x* axis is the radius of the lipid disk within a DMPC/apo A-I complex. Add 15 Å to obtain the radius of the entire discoidal complex.

by apparently continuous changes in the Stokes diameter with concentration for the smallest of the R-2 species in the concentration range below 200 M/M DMPC/apo A-I (see Figure 5). This continuous size variation seems likely to be due to some flexibility in the lateral packing of amphipathic helices and/or phospholipid head groups within the DMPC/apo A-I complex.

We have previously shown for SUV that the inner monolayer choline *N*-methyl proton resonance is a sensitive indicator of SUV size in general and head group surface area in particular (Brouillette et al., 1982). We were interested in determining what effect the molecular organization of the phospholipid/apo A-I complex would have on the *N*-methyl resonance and if it could be used to distinguish between the different micellar classes. As illustrated in Figure 4 and 8B (insert), the choline *N*-methyl resonance can be used to distinguish between a vesicular structure and a micelle. It is interesting to note that the inner monolayer choline *N*-methyl resonance of the vesicular complexes formed at a 700 DMPC/apo A-I molar ratio is significantly downfield compared to the inner monolayer choline *N*-methyl resonance of DMPC SUV: 3.254 vs. 3.240 ppm, respectively. Of several possible explanations which would be consistent with binding of the protein to the outer monolayer, the simplest invokes our knowledge of the relationship between vesicle size and chemical shift of the inner monolayer choline *N*-methyl resonance. One may envision that the added outer monolayer surface area in the presence of apo A-I has caused a growth of the vesicle and, in this case, a downfield shift of the inner monolayer *N*-methyl resonance would follow. The exact molecular mechanism by which this shift occurs (e.g., changes in head group hydration or conformation) is unknown and presently under investigation.

With respect to the micellar complexes, the chemical shift of the micelle *N*-methyl resonance is indicative of the size of the micelle by its relationship to the DMPC/apo A-I molar ratio (see Figure 3F). In Figure 6, the micelle *N*-methyl resonance is seen to shift downfield with increasing DMPC/apo A-I ratio. We known from several different techniques that there is also a concomitant increase in the average size of the micellar complex produced. Illustrated in Figure 12A is a plot of the micelle *N*-methyl chemical shift vs. the DMPC/apo A-I molar ratio from which the complex was produced. The relationship is clearly nonlinear. It is unlikely that a specific protein–lipid interaction is solely responsible for the change in chemical shift because we also have observed a direct relationship between micelle size and chemical shift in egg PC/deoxycholate micelles (Brouillette et al., 1982). Due to the discoidal morphology of both the DMPC/apo A-I and the egg PC/deoxycholate complexes, the data can be interpreted in terms of a difference between the chemical environment of the lipid around the perimeter of the disk and the lipid which is in direct contact with only other lipid molecules, that is, core lipid. The observed chemical shift of the micellar choline *N*-methyl resonance is then a weighted average of the two head group environments. In support of this interpretation is the curve depicted in Figure 12B. This curve illustrates how the percent surface area of the disk core (9 Å is taken as the cross-sectional diameter of a single DMPC molecule) varies as a function of the radius of the disk and is relevant only if apo A-I is located exclusively around the perimeter of the disk. Since there is a direct relationship between surface area and number of lipid molecules, this curve reflects the fraction of DMPC molecules in the disk core of a given disk radius.

Our data on DMPC/apo A-I micellar complexes are most compatible with the formation of micelles containing either two (R-2) or three (R-3) apo A-I molecules per particle. It is interesting that smaller particles with a stoichiometry of one apo A-I molecule per particle (R-1) are not observed (Swaney, 1980). On the basis of surface area considerations, the 40 molar ratio egg PC/apo A-I complexes formed by detergent dialysis are small enough (diameter = 74 ± 10 Å) to exist with only one apo A-I molecule per particle. However, preliminary cross-linking experiments on isolated complexes (unpublished results) do not support this interpretation. Interestingly, chemical analyses of isolated HDL subspecies (unpublished experiments) are consistent with an apo A-I stoichiometry of 2 for the smallest particles (Diameter = 80 Å). From these observations, it is possible that the apo A-I conformation in the egg PC/apo A-I and HDL complexes is significantly different from that in the DMPC/apo A-I complexes.

The overall size distribution of complexes produced between apo A-I and phosphatidylcholines belies an apparently restrictive mechanism for their formation. Not only is the apo A-I stoichiometry of the complex highly controlled but also the species within a given stoichiometric class of particles are discretely sized in a manner compatible with conservative changes in the lipid-associated A-I conformation. The physical state and fatty acyl chain conformation of DMPC within apo A-I complexes have been shown by calorimetry (Tall et al., 1977; Gilman et al., 1981) and Raman spectroscopy (Gilman et al., 1981) to be distinctly different from those for DMPC

MLV. Our ^1H NMR studies on the DMPC/apo A-I discoidal micelles indicate that the chemical environment around the phosphatidylcholine head groups located at the perimeter of the disk is also distinctly different from that for DMPC vesicles. We are currently investigating the molecular mechanisms for the chemical shift differences between disk core and perimeter lipids. In a later paper, we will present evidence which suggests that the discrete nature of HDL subpopulations may be at least partially understood in terms of the mechanisms proposed here to explain phospholipid/apo A-I recombinant size flexibility.

Acknowledgments

We are indebted to Dr. Charles Schmidt for many helpful discussions and suggestions and his critical reading of the manuscript. C.G.B. is very grateful for the expert technical instruction by Sharon Frase in negative stain electron microscopy. We also thank Barbara Schmidt for typing the manuscript.

References

Atkinson, D., Smith, H. M., Dickson, J., & Austin, J. P. (1976) *Eur. J. Biochem. 64*, 541.

Atkinson, D., Small, D. M., & Shipley, C. G. (1980) *Ann. N.Y. Acad. Sci. 348*, 284.

Blanche, P. J., Gong, E. L., Forte, T. M., & Nichols, A. V. (1981) *Biochim. Biophys. Acta 665*, 408.

Brouillette, C. G., Segrest, J. P., Ng, T. C., & Jones, J. L. (1982) *Biochemistry 21*, 4569.

Campbell, I. D., Dobson, C. M., Williams, R. J. P., & Xavier, A. V. (1973) *J. Magn. Reson. 11*, 172.

Edelstein, C., Lim, C. T., & Scanu, A. M. (1973) *J. Biol. Chem. 247*, 5842.

Forte, T. M., Nichols, A. V., Gong, E. L., Lux, S., & Levy, R. I. (1971) *Biochim. Biophys. Acta 248*, 381.

Gilman, T., Kauffman, J. W., & Pownall, H. J. (1981) *Biochemistry 20*, 656.

Green, R. H. R., Tall, A. R., & Glickman, R. M. (1978) *J. Clin. Invest. 61*, 528.

Hamilton, R. L., Williams, M. L., Fielding, L. J., & Havel, R. L. (1976) *J. Clin. Invest. 58*, 677.

Jonas, A., Krajnovich, D. J., & Patterson, B. W. (1977) *J. Biol. Chem. 252*, 2200.

Jonas, A., Drengler, S. M., & Patterson, B. W. (1980) *J. Biol. Chem. 255*, 2183.

Jonas, A., Drengler, S. M., & Kaplan, J. S. (1981) *J. Biol. Chem. 256*, 2420.

Kane, J. P. (1973) *Anal. Biochem. 53*, 350.

King, J., & Laemmli, U. K. (1971) *J. Mol. Biol. 162*, 465.

Lowry, O. H., Rosebrough, N. J., Farr, A. L., & Randall, R. J. (1951) *J. Biol. Chem. 193*, 265.

Matz, C. E., & Jonas, A. (1982a) *J. Biol. Chem. 257*, 4535.

Matz, C. E., & Jonas, A. (1982b) *J. Biol. Chem. 257*, 4541.

Middelhoff, G., Rosseneu, M., Peeters, H., & Brown, M. V. (1976) *Biochim. Biophys. Acta 441*, 57.

Morrisett, J., Jackson, R., & Gotto, A., Jr. (1977) *Biochim. Biophys. Acta 472*, 93.

Nichols, A. V., Gong, E. L., Blanche, P. J., & Forte, T. M. (1983) *Biochim. Biophys. Acta 750*, 353.

Norum, K. R., Glomset, J. A., Nichols, A. V., Forte, T. M., Albers, J. J., King, W. C., Mitchell, C. D., Applegate, K. R., Gong, E. L., Cabana, V., & Gjone, E. (1975) *Scand. J. Clin. Lab. Invest., Suppl. 35 (No. 142)*, 31.

Pownall, H. J., Massey, J. B., Kusserow, S. K., & Gotto, A. M., Jr. (1978) *Biochemistry 17*, 1183.

Pownall, H. J., Van Winkle, W. B., Pao, Q., Rohde, M., & Gotto, A. M., Jr. (1982) *Biochim. Biophys. Acta 713*, 494.

Segrest, J. P. (1977) *Chem. Phys. Lipids 18*, 7.

Segrest, J. P., & Feldmann, R. J. (1977) *Biopolymers 16*, 2053.

Segrest, J. P., Jackson, R., Morrisett, J., & Gotto, A., Jr. (1974) *FEBS Lett. 38*, 247.

Segrest, J. P., Pownall, H. J., Jackson, R. L., Glenner, G. G., & Pollock, P. S. (1976) *Biochemistry 15*, 3187.

Stewart, J. C. M. (1980) *Anal. Biochem. 104*, 10.

Swaney, J. B. (1980) *J. Biol. Chem. 255*, 877.

Swaney, J. B., & Chang, B. C. (1980) *Biochemistry 19*, 5637.

Tall, A. R., Small, D. M., & Shipley, G. G. (1977) *J. Biol. Chem. 252*, 4701.

Wetterau, J. R., & Jonas, A. (1983) *J. Biol. Chem. 258*, 2637.

Wlodawer, A., Segrest, J. P., Chung, B. H., Chiovetti, R., Jr., & Weinstein, J. N. (1979) *FEBS Lett. 104*, 231.